Available online www.jsaer.com

***Journal of Scientific and Engineering Research*, 2019, 6(7):212-228**

Research Article

ISSN: 2394-2630
CODEN(USA): JSERBR

Prediction of Rutting for Local Soil Mixes with Emulsified Sulfur Asphalt and Emulsified Asphalt

Yasser M. Alghrafy[1]*, El-Sayed M. Abdellah[2]

[1]Demonstrator, Civil Engineering Department, Faculty of Engineering, Sana'a University, Sana'a, Yemen
[2]Professor of Highways and Airports Engineering, Civil Engineering Department, Faculty of Engineering, Assuit University, Assuit, Egypt
*Corresponding author. Email:alghrafy@gmail.com

Abstract The primary aim of this study is to assess the engineering properties of asphalt emulsion (EA) and 30/70 sulfur modified emulsified (ESA) asphalt treated mixtures for their potential applications in roads. Also generate rutting models which have been obtained to predict the permanent strain in the base using VESYS model.

The test procedure conducted on three types of soils that cover an important geographical area of the Kingdom of Saudi Arabia, marl, dune sand, and sabkha. The design mixtures were subjected to Marshall Stability test, Tensile strength test, Resilient Modulus (MR) test, and Static triaxial test. Whereas, the behavior of mixes under dynamic loads were studied using dynamic triaxial test.

The results showed that resilient modulus has improved for sabkha soil with ESA but this impact was negative with marl and dune sand. Moreover, ESA blend shows lower water absorption compared to their EA blend. Durability has increased when ESA was used compared of EA. The use of the ESA slightly reduced the value of permanent deformation for mixtures with sabkha. While it has a negative impact on the ability to resist collapse time. Permanent deformation has increased when the ESA was used with marl and dune sand compared of EA.

The results from both the permanent deformation test and VESYS model results have been used in developing design charts and guidelines for the selection of a base thickness for the allowable traffic.

Keywords VESYS model, asphalt emulsion, Emulsified Sulfur Asphalt, permanent deformation, Resilient Modulus, dynamic loads, design charts

Introduction

The most premature failures of asphalt pavement are permanent deformation which defined as the accumulation of plastic deformation due to continuous repeated loads from traffic loading. Plastic deformation happens more often than before with the increase of traffic nowadays. One of the widely used tests is the simulation laboratory test using the repeated load test.

Most important parts of Saudi Arabia are covered with the dune sand which is characterized as poorly graded soil with high permeability. In addition to that, marl and sabkha are available in some parts in Saudi Arabia, which have a poor strength to change their properties with water. But in some cases, it is usually required to use these materials as sub-grade layers or as a backfill in base and sub-base layers of roads and highways so some kind of stabilization is required to improve the characteristics of these materials.

Emulsified asphalt provides an easy means of stabilizing dunes for protection of roads and industrial areas. Moreover, emulsified asphalt can be used for preparation of industrial sites. Therefore, emulsified asphalt appears to be attractive for use in Saudi Arabia and deserving of further study [1].

The repeated load test has proven to be a feasible alternative in evaluating rutting and test results can be used as predictive measures to analyse the performance of emulsified asphalt soil mixture in road conditions. There are two main, mechanisms responsible for permanent deformation in bituminous materials, densification and Shear displacement. Compaction phase is where the soil particles become more closely serried and can be a problem in pavements which are poorly compacted during construction. This phase tends to happen comparatively early in the life of a pavement structure. The other phase is shear displacements which tend to flow of material in a constant volume process and happen during the life of the pavement structure [2].

Materials and Methods

Raw Materials

Three types of soils were selected for this study, non-plastic marl, dune sand and sabkha. The Sabkha was collected from Al-Aziziyah zone, which is located 10 km south of Dhahran, Saudi Arabia. Marl and dune sand were chosen due to their abundance at low cost in Saudi Arabia. It was collected from Dhahran city. The asphalt emulsion (EA) used in this study is the only locally available grade CSS-1h, obtained from
SANDFIX Company and the Emulsified Sulfur Asphalt (ESA) was produced using the laboratory Emulsified Asphalt plant available in KFUPM laboratory.

Experimental Design

Soil characterization

To investigate the probable treatment of these soils and their use in the construction of road projects, physical property tests were performed. These Physical tests included Liquid Limit, Plastic Limit, Specific Gravity, Relative Density tests and grain size distribution. The compaction and strength characteristics were investigated by using modified Proctor compaction and California bearing ratio tests. Table 1 shows the various tests performed on each soils along with the test designations from ASTM Specifications [3].

Table 1: Soils Physical Properties

Test	Marl	Dune sand	Sabkha
Specific Gravity	2.68	2.63	2.47
Dry Density, kN/m^3	18.4	---	17.1
Optimum Water content, %	13	9	12
Minimum density	---	1.63	---
Maximum density	---	1.84	---
California Bearing Ratio (CBR), %	25	15	10
AASHTO	A-1-b	A-3	A-3
USCS system	SM	SP	SP-SM

Optimization of stabilized soils

The modified Marshall Mix design method was employed to prepare the test specimens.
The purpose of the mix design is to find the optimum emulsified sulfur asphalt and optimum emulsified asphalt.
The Cold Mixture Design method according to A Basic Asphalt Emulsion Manual [4] was used for mixing the EA and ESA with soil. It was used to determine the optimum EA and ESA content for dune sand, marl and Sabkha. Thus mix trials were made for different emulsion ranges (3% to 18% of dry soil's weight). Water added was varied between 1% and 5%. A 2% Portland cement was added for early curing. Mixing time was limited to (30) seconds to avoid stripping problem. The product mix was compacted using the Marshall compactor; where 75 blows applied to each side The compacted specimens, after curing for 48 h in an oven at 60 ^{o}C, were tested using Marshall stability test at 25 ^{o}C for dry samples and after soaking for 2 h at 25 ^{o}C for wet samples to determine durability.

Evaluation of designed mixes

Marshall stability, ITS (indirect tensile strength), and Static triaxial tests were carried out at temperatures of 22°C while, MR (Resilient Modulus) and Dynamic triaxial tests were carried out at temperatures of 22°C and

40°C. All tests were done following ASTM [3] and AASHTO [5] Standards. A flow chart of the experimental design and the experimental design are shown in Figure 1 and Table 2, respectively.

Table 2: Experimental Design

Test	Temperature, °C	EA or ESA%
Marshal Stability	22	
	---	3 to 18
Indirect tensile strength	22	
Static triaxial	22&40	At optimum
Resilient modulus	22&40	At optimum
Dynamic triaxial	22&40	

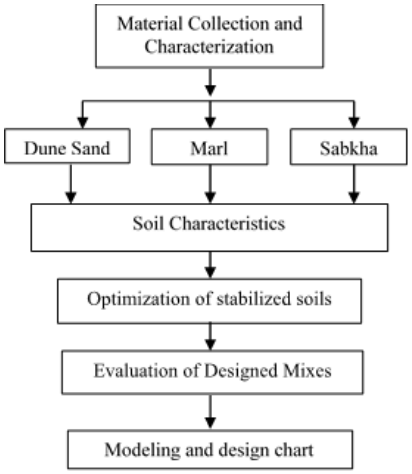

Figure 1: Flow chart of the experimental design

Results & Discussion

The results of the emulsified sulfur asphalt mix design indicated that the optimum residual emulsified sulfur asphalt content for the marl is 7.2 %, 3.6 % for sabkha and 5.4 % for the dune sand. While the results of the emulsified asphalt mix design indicated that the optimum residual emulsified asphalt content for the marl is 8 %, 4 % for sabkha and 5.4 % for the dune sand.

The results of durability indicated that marl, sabkha and dune sand mixes at optimum residual emulsion sulfur asphalt and optimum residual emulsion asphalt have a more than 50% (minimum durability 50%)[6]. EA blends showed lower durability compared to their ESA blends for marl and sabkha.

For all mixes the results of water absorption showed that at optimum residual emulsion sulfur asphalt and optimum residual emulsion asphalt have a less than 4% (maximum allowable value for the water absorption is 4 %) [6]. ESA blend shows lower water absorption from 30% to 80% compared to their EA blend.

ITS results for marl and sabkha with EA and ESA at optimum residual asphalt content satisfies the recommended requirements of 200 kPs [6], but the ITS for dune sand mixes did not exceed the minimum requirement of ITS. Summary of marshal, durability, water absorption, and ITS are shown in Table 3.

Table 3: Summary of results for marshal stability

Soil type	Type of additive	optimum residual asphalt%	Dry Stability (kN)	Soaked Stability (kN)	Water absorption %	Durability %	ITS (KPa)
Marl	EA	8.0	33.0	29.4	0.80	90	615
	ESA	7.2	22.4	19.8	0.68	91	617
Sabkha	EA	4.0	12.5	7.50	1.30	60	233
	ESA	3.6	10.6	6.80	0.88	65	270
Dune	EA	5.4	12.0	7.00	0.37	85	163
Sand	ESA	5.4	9.80	5.30	0.71	54	106

The triaxial test results were used to plot Mohr-Coulomb envelopes, from which angle of internal friction (φ), cohesion (C) and shear strengths were determined. The Mohr-Coulomb failure criterion was used to establish the relation between these parameters. Table 4 summarizes the test parameters for marl, sabkha and dune sand.

Table 4: Shear parameter for Mohr-Coulomb failure envelope of treated soils

Treatment type	Soil Type	Angle of Internal Friction	Cohesion (KPa)
Emulsified Asphalt	Marl	27	292.5
	Sabkha	33	14.8
	Dune Sand	30	25
Emulsified Sulfur Asphalt	Marl	33	134
	Sabkha	30	15
	Dune Sand	31	11.4

In the resilient modulus test, three specimens were tested for each material at a temperature 22°C and 40°C. Summary of resilient modulus at 22°C and 40°C temperatures are shown in Table 5 and Table 6 respectively.

Table 5: results of resilient modulus (MPa) at 22°C

Type of additive		EA			ESA		
Confining stress (kPa)	**Deviator stress (KPa)**	**sand**	**marl**	**sabkha**	**sand**	**marl**	**sabkha**
20.68	34.47	226	272	255	170	257	274
	48.26	235	281	232	174	257	273
	68.94	280	307	281	213	295	295
34.47	34.47	239	296	277	186	266	286
	68.94	309	301	310	247	362	335
	103.42	452	419	457	365	483	461
68.95	34.47	253	264	287	146	224	280
	68.94	302	323	334	304	358	318
	137.90	580	587	616	561	674	611
	206.84	846	1028	968	827	975	952
103.4	68.94	300	307	314	295	330	324
	137.9	575	617	663	530	689	622
	206.84	919	1014	925	870	973	925
	275.79	1101	1369	1141	1150	1355	1239
137.9	68.94	322	336	294	278	328	301
	103.42	436	465	414	417	492	442
	137.9	601	648	614	524	660	593
	206.84	907	892	898	832	997	931

Table 6: Results of resilient modulus (MPa) at 40°C

Type of additive		EA			ESA		
Confining stress (kPa)	**Deviator stress (KPa)**	**sand**	**marl**	**sabkha**	**sand**	**marl**	**sabkha**
20.68	34.47	200	242	216	212	154	186
	48.26	196	286	229	216	246	230
	68.94	243	283	289	256	320	272
34.47	34.47	204	271	205	214	178	200
	68.94	262	289	269	267	350	296
	103.42	401	427	410	423	490	458
68.95	34.47	212	174	156	166	200	223
	68.94	278	332	290	284	313	289
	137.90	540	589	579	600	637	638
	206.84	783	932	826	853	940	880
103.4	68.94	253	275	257	276	305	293
	137.9	503	565	533	558	648	614
	206.84	804	916	843	862	911	890
	275.79	1037	1271	1092	1148	1291	1198
137.9	68.94	262	296	265	293	296	283
	103.42	367	426	393	411	441	409
	137.9	529	593	529	538	631	576
	206.84	773	900	875	800	960	830

From Table 5 and Table 6, it can be seen that the MR at 22^{o}C and 40^{o}C is increased considerably with increasing deviator stress with good regression correlation. Also, marl produced a higher MR relative to the other soil and the MR of the sabkha was higher than that of dune sand at 22^{o}C and 40^{o}C. The results show that the addition of EA to marl and dune sand reduce the MR significantly as compared ESA because the fact that sulfur prevents water evaporation during the curing stage. The reduction for marl was about 20% and 15% for Sabkha depending on the applied deviator stress.

For effect of temperature on MR, we can see that increasing the temperature causes lower the modulus of resilience because mix tends to lose its Stiffness by softening with an increasing the elastic deformation and hence a decrease in the MR value.

Finally, for Permanent deformation tests, Permanent deformation tests were accomplished on the treated marl, sabkha, and dune sand specimens to evaluate the permanent deformations under dynamic loading condition. The effects of various deviator stress (137.8 to 551.5 kPa) and stabilizer type (EA and ESA) at 22°C and 40°C temperature on the permanent deformations were studied for all soils and additive combinations. Three samples of each material treated and combinations were tested for each temperature, the total number of samples were 138.

To study permanent deformation behaviour under repeated loads for soils mixer with EA and ESA, the shakedown theory was applied. This theory holds that, the permanent deformation behaviour of pavement materials steadily stabilizes as the number of load cycles increases, making it possible to define a limit value for the accumulation of permanent strain. This stabilization is only reached when the applied stresses are low, given that high stresses would result in the continuous growth of permanent stress and gradual deterioration [6]. The test results were plotted for vertical permanent strain as ordinate and number of load repetitions as horizontal coordinate. The corresponding deformation compliance curves for the rest of the mixtures are given from Figure 2 to Figure 13. It can be seen from these figures that the deformation compliance curve versus loading time can be divided into three distinct regions: primary Stage (range A), where the samples compact an initial amount during the very first load cycles and the strain rate decreases, secondary Stage (range B) where they usually continue to compact gradually over many load cycles and the strain rate is constant, and the tertiary Stage (range C) where the strain rate increases.

The deformation curve in the secondary stage region is plotted as a straight line on a log–log scale so it is also referred to as linear deformation. In this phase the material is considered to be in behavioural ‘‘range B”. This linear deformation continues indefinitely and the material does not reach failure. However, when a higher stress or with a greater number of load cycles are applied the permanent deformation is more elevated and the material might enter into ‘‘range C” behaviour and, finally, reach failure. Lastly, if the applied stress is even higher, the permanent strain accumulates rapidly in a low number of load cycles. In this condition the material will reach failure and rutting will take place very quickly. In this phase the material is in behavioural ‘‘range C”.

The stress levels in this test were selected on the basis of the stresses supported by a well-designed, constructed section of pavement of low traffic to high traffic roads [7]. Therefore, according to the shakedown concept [6], if the section is well-designed, its pavement structural behaviour should be in stable conditions, i.e., it should be within at the most, in ‘‘range B”.

In this way, for blends with ESA, Figure 2 shows that marl with ESA at 22°C at stress 551.5 kPa behaved as in ‘‘range B”. However, when N increases, it has given rise to an increment in permanent deformation. It is possible that if a higher N were applied, the material might pass over to ‘‘range C”. While at stress levels 482.6, 275.8, and 137.8 kPa, it behaved as in ‘‘range B”.

Figure 3 shows that, as regards stress levels 551.5, 482.6, and 413.6 kPa, marl with ESA at 40oC behaved as in ‘‘range B”. This behaviour continued indefinitely and the material did not reach a failure stage.

Figure 4 and Figure 5 show that, at stress levels 551.5, 482.6, and 413.6 kPa, sabkha with ESA at 22°C behaved as in ‘‘range B” but with a greater number of load cycles, the material might enter into ‘‘range C” behaviour and, finally, reach failure. While, at stress levels 551.5, 482.6, and 413.6 kPa, sabkha with ESA at 40°C behaved as in ‘‘range B” but it was continued indefinitely and the material does not reach failure.

Figure 6 shows that, at stress levels 413.6, 482.6 and 551.5 kPa, dune sand with ESA at 22°C behaved as in ‘‘range c” because the applied stress was even higher and the permanent strain accumulated rapidly in a low

number of load cycles. In this condition the material was reached failure. While, at stress 275.8 kPa, it behaved as in ‘‘range B”. Also in Figure 7, dune sand with ESA at 40°C and stress levels 482.6, and 551.5 kPa exhibited a trend in much the same way as dune sand at 22°C and stress levels 482.6, and 551.5 kPa, but reaches a failure stage at the high number of repetitions.

As a conclusion from permanent deformation results for soil with ESA, when the applied axial stress increased, the magnitude of the axial permanent strain accumulation increased. The increase in strain was very significant at high stresses, whereas low strains were accumulated at low stress levels. This implies that the asphalt mix would experience considerable amount of permanent deformation under high wheel loads from vehicles in the field, hence significant rutting is expected under such a condition.

For soil with EA, Figure 8 and Figure 9 show that in the samples for marl with EA at 22^{o}C and 40^{o}C respectively, with all stress levels, the increase was a little more accentuated. This deformation increase continues indefinitely and the material does not reach failure so the material exhibits a ‘‘range B” behaviour.

Figure 10 and Figure 11 show that, as regards stress levels 551.5, 482.6, and 413.6 kPa, sabkha with EA at 22^{o}C and 40^{o}C respectively behaves as in ‘‘range B”. However, when N increased, it has given rise to an increment in permanent deformation and the material might pass over to ‘‘range C”. While at stress levels 275.8, and 137.8 kPa, sabkha with EA at 22^{o}C behaved as in ‘‘range B” because it did not pass over to ‘‘range C”.

Figure 12 shows that, at stress levels 137.8, 275.8, and 413.6 kPa, dune sand with EA at 22^{o}C behaved as in ‘‘range B”. However, when N increases it gives rise to an increment in permanent deformation and the material might pass over to ‘‘range C”. While at stress levels 482.6, and 551.5 kPa, sabkha with EA at 22^{o}C behaves as in ‘‘range c” because the applied stress was even higher, the permanent strain accumulates rapidly in a low number of load cycles. In this condition the material was reached failure and rutting was taken place very quickly. Also in Figure 13, dune sand with EA at 40^{o}C and stress levels 413.6, 482.6, and 551.5 kPa exhibited a trend in much the same way as dune sand at 22^{o}C and stress levels 482.6, and 551.5 kPa, but it reached a failure stage at low number of repetitions.

As a conclusion from permanent deformation results for soil with EA, when the applied axial stress increased, the magnitude of the axial permanent strain accumulation increased. The increase in strain was very significant at high stresses and high temperatures, whereas low strains were accumulated at low stress levels and temperatures. This implies that the asphalt mix would experience considerable amount of permanent deformation under high wheel loads from vehicles at high temperatures in the field, hence significant rutting is expected under such a condition.

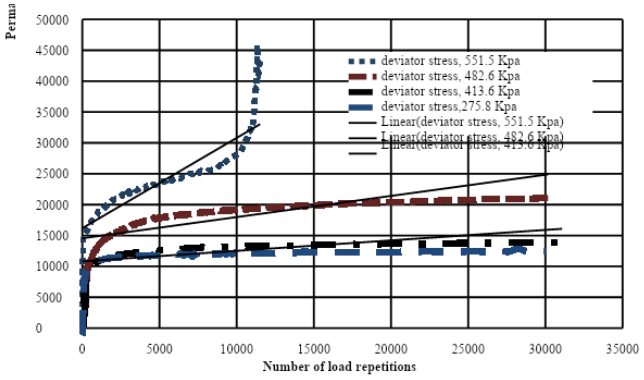

Figure 2: Evolution of permanent axial strains with the number of load cycles for marl with ESA, for different levels of deviatoric stress at 22^{o}C

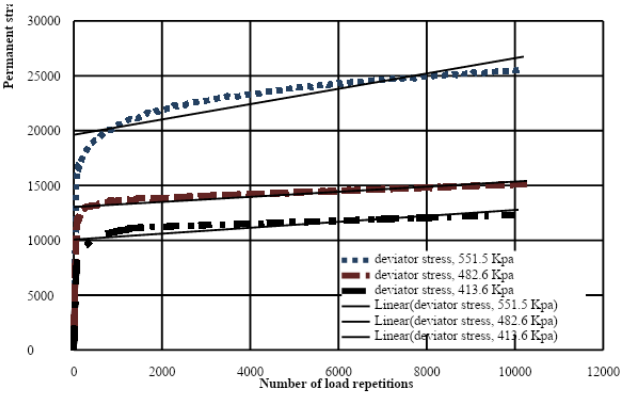

Figure 3: Evolution of permanent axial strains with the number of load cycles for marl with ESA, for different levels of deviatoric stress at 40^{o}C

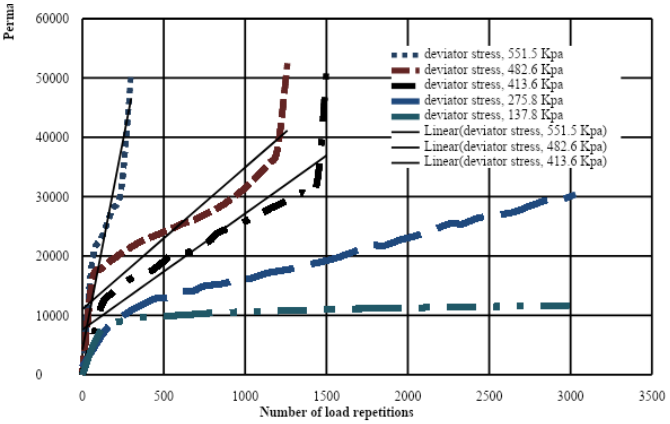

Figure 4: Evolution of permanent axial strains with the number of load cycles for sabkha with ESA, for different levels of deviatoric stress at 22°C

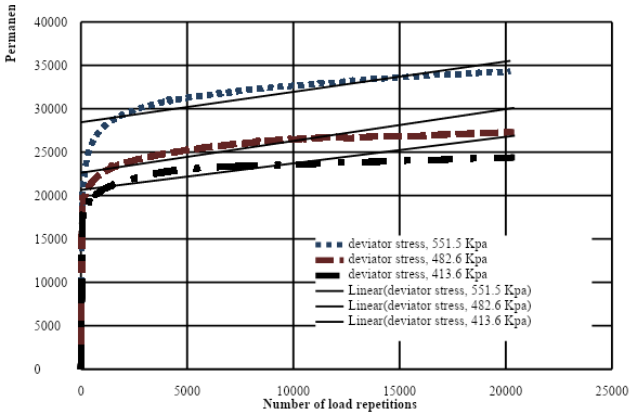

Figure 5: Evolution of permanent axial strains with the number of load cycles for sabkha with ESA, for different levels of deviatoric stress at 40°C.

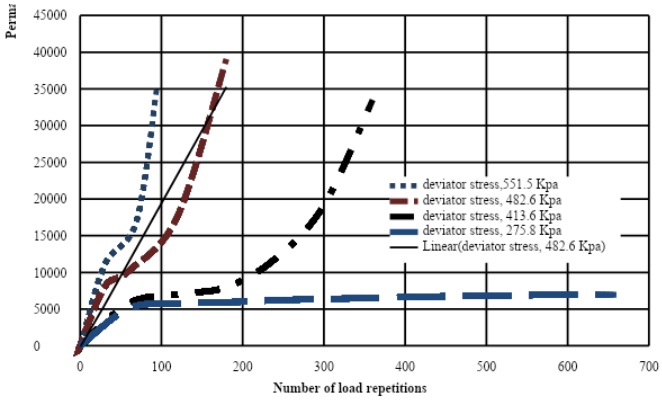

Figure 6: Evolution of permanent axial strains with the number of load cycles for dune sand with ESA, for different levels of deviatoric stress at 22°C

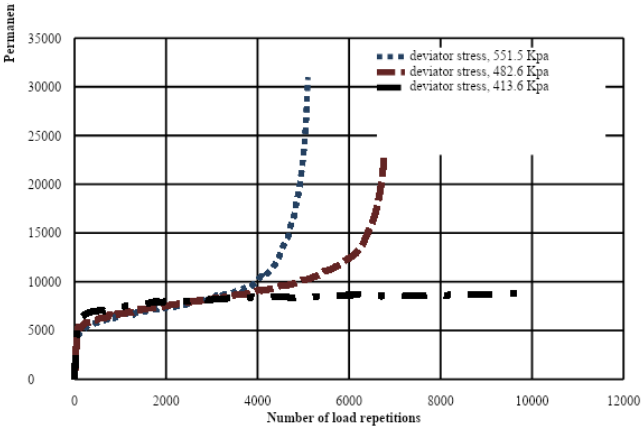

Figure 7: Evolution of permanent axial strains with the number of load cycles for dune sand with ESA, for different levels of deviatoric stress at 40°C

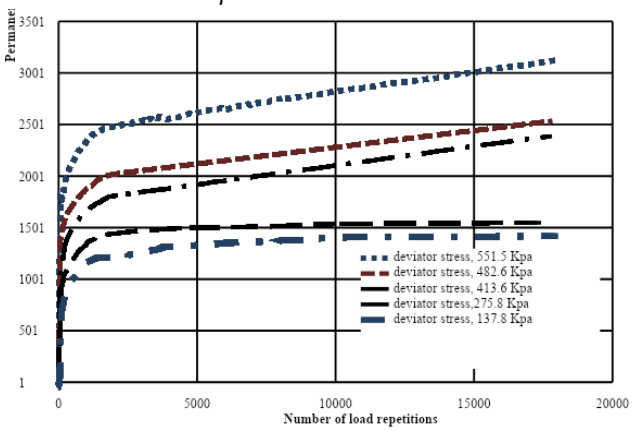

Figure 8: Evolution of permanent axial strains with the number of load cycles for marl with EA, for different levels of deviatoric stress at 22°C

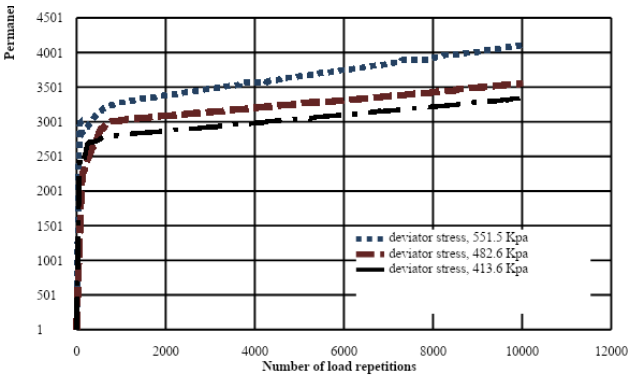

Figure 9: Evolution of permanent axial strains with the number of load cycles for marl with EA, for different levels of deviatoric stress at40°C

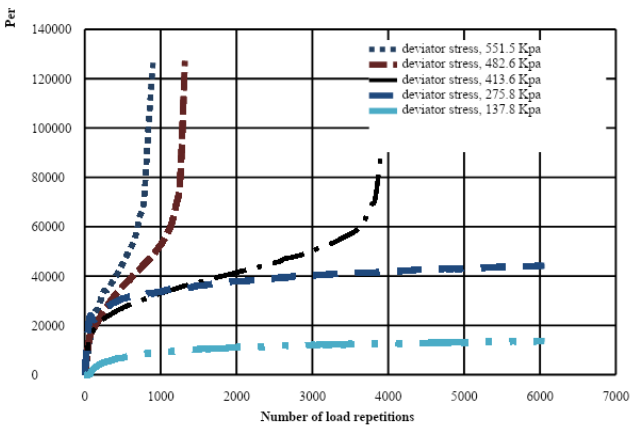

Figure 10: Evolution of permanent axial strains with the number of load cycles for sabkha with EA, for different levels of deviatoric stress at 22^{o}C

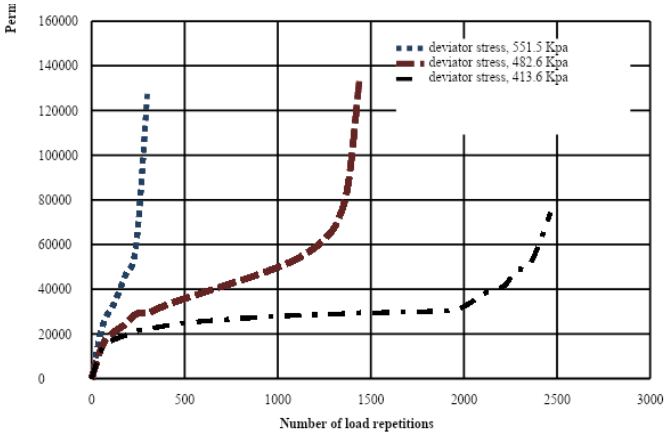

Figure 11: Evolution of permanent axial strains with the number of load cycles for sabkha with EA, for different levels of deviatoric stress at 40^{o}C

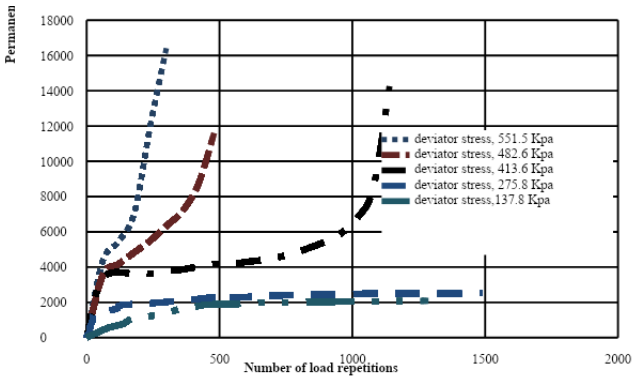

Figure 12: Evolution of permanent axial strains with the number of load cycles for dune sand with EA, for different levels of deviatoric stress at 22^{o}C

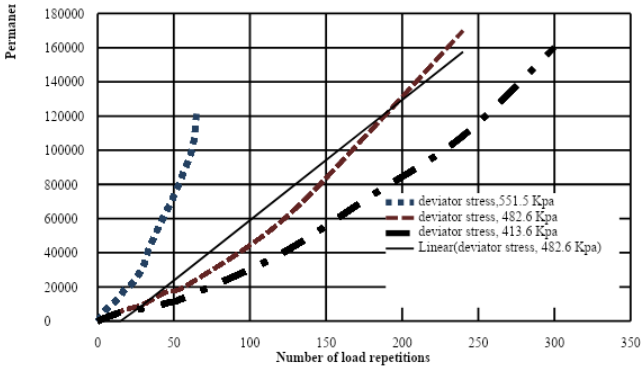

Figure 13: Evolution of permanent axial strains with the number of load cycles for dune sand with EA, for different levels of deviatoric stress at 40^{o}C.

When comparing the permanent deformation between of soil with EA and soil with ESA, we can see three ways, effect of loads or stress, effect of temperature and effect of type of additive. Firstly, EA bends and ESA bends have the same rutting behavior when increasing or decreasing the stress levels where the rutting increased with increase stress. Secondly, for all blends containing EA additives when testing at 40 °C; the permanent axial strain was increased when increasing temperature while for all blends containing ESA additives, the permanent axial strain was decreased when increasing temperature. That's because, particles of sulfur in ESA dissolve with increasing temperature and lead to eliminating the voids so density and rutting resistance are increased. Finally, Treatment of sabkah and dune sand soil with ESA increased the permanent axial strains and decreased the number of repetitions significantly compared when EA was added. Marl exhibits a trend in much the same way as sabkha and dune sand, but does not reaches it's a tertiary stage.

The Permanent deformation results for three subgrade soils are shown in Figure 14. Marl and sabkha, soils were mixed with the optimum water content. Then mixed samples were fabricated to specimens of 200 mm diameter by 400 mm height. Each specimen was compacted to the corresponding density obtained in the proctor compaction test. For dune sand, Specimens were prepared by vibratory compaction methods using a vibration Table. Three samples for each soil were prepared and cured at 22°C for 72 hours and tested dry under a repeated load for confining stress of 69 kPa and deviatoric stress of 138kPa at 22oC. Results indicate that, Marl produced a higher resistance to deformation relative to the soil materials and the resistance to deformation of the sabkha was found to be higher than that of the dune sand.

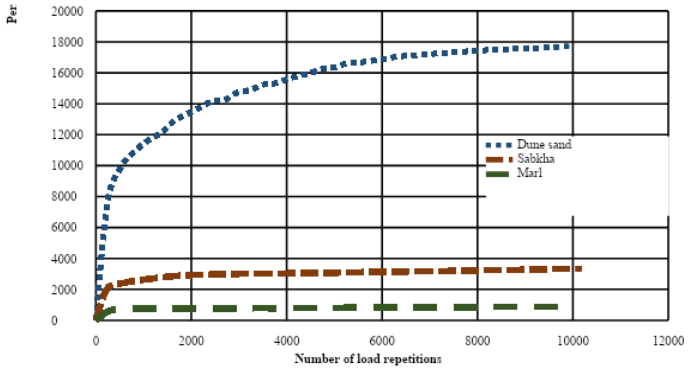

Figure 14: Evolution of permanent strains for subgrade soil.

Model

Rutting Model

The model adopted in this study is the rutting model of VESYS [8], a computer program package developed for the Federal Highway Administration, U.S.A. The concept of VESYS for rut prediction is based on the assumption that permanent strain is proportional to the resilient strain in the formula:

$$\varepsilon_p = \mu \varepsilon_r N^{-\alpha} \quad (1)$$

Where: ε_p = the permanent or plastic strain due to a single load application, μ = a permanent deformation parameter representing the constant of proportionality between permanent strain and elastic strain, εr = resilient strain, N = load applications, α = a permanent deformation parameter indicating the rate of decrease in the rutting parameters μ and α, are defined by:

$$\mu = \frac{ab}{\varepsilon_r}, \quad \alpha = 1 - b \quad (2)$$

The data from the permanent defamation test was used to establish a rutting model. There are three treatment soil marl, sabkha and dune sand with EA and ESA additive which using as constriction base material. To predict the rutting model, pavement system and traffic characteristics were selected. After that, the response of the pavement in terms of stresses was computed using the 3D-MOVE analysis computer program [9]. Then pavement Materials Properties (ie, resultant modulus) were computed from test results. Finally, layer rutting was carried using TTI VESYS5W [10].

Pavement systems (cases analyzed)

Two types of pavement structure were simulated using VESYS model. The first structure is a conventional flexible pavement for local streets consisting of asphalt concrete as the surface layer 5cm, improved marl soils by EA and ESA as the base, and the local soil subgrade. This structure consists of two cases as shown in Figure 15.

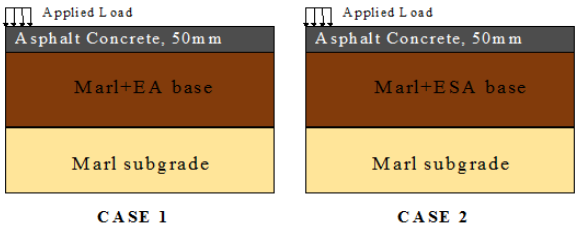

Figure 15: Pavement structures on marl subgrade.

The second structure is similar to the first structure, but the number of layers are four with additional subbase layer. This system is used when subgrade is sabkha or dune sand. The use of Subbase below the base in this system serve as the foundation for the total pavement structure, transferring traffic loads to the subgrade, providing drainage and frost protection. In addition to this, Since CBR of subgrade (dune sand and sabkha) is between 10% and 15%, 150 mm thickness subbase layer is used [11]. This structure consists of eight cases as shown in Figure 16 and Figure 17.

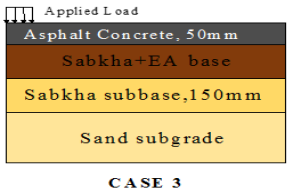

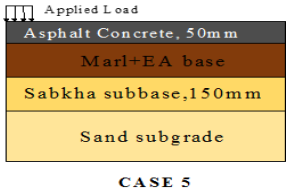

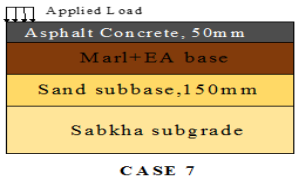

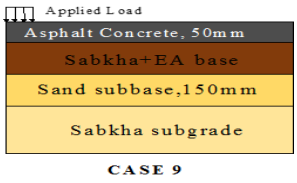

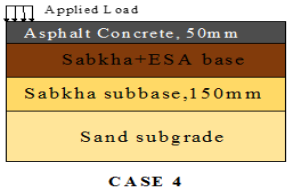

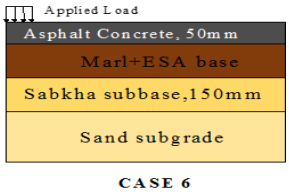

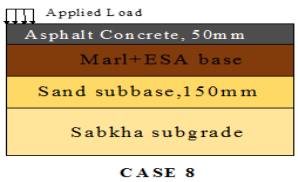

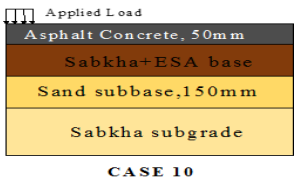

Figure 16: Pavement structures on sand subgrade *Figure 17: Pavement structures on sabkha subgrade*

Traffic characteristics

The traffic characteristics are determined in terms of the number of repetitions of an 80 kN single-axle load applied to the pavement on two sets of dual tires. The dual tires are represented as two circular plates, each 11.5 cm in diameter, spaced 34.5 cm apart. This representation corresponds to a contact pressure of 482.6 kPa [7].

Multilayer linear elastic systems analyses

The pavement system is subdivided into number of sublayers. Each sublayer is assigned an initial resilient modulus from the resilient modulus test, and in each sublayer locations for stress computations are defined. The 3D-MOVE analysis computer program [9] computes the state of stress at all locations in each sublayer, then averages them, and computes a new value of the resilient modulus for each sublayer, using results of resilient modulus test. This analysis is interactive until the deviation between two consecutive computed resilient modulus is less than 1% in all sublayers.

Pavement Materials' Properties

For subgrade layer, the Material Properties is normally characterized by CBR test, although predict the rutting model requires resilient modulus as the input data. The most widely relation between CBR and resilient modulus used for the subgrade stiffness is the following relations as determined by Heukelom and Klomp [12]

$M_R = 10.34 \times CBR, \quad CBR \leq 10\%$ (3)

$M_R = 20.68 \times CBR^{0.65}, \quad CBR > 10\%$ (4)

For base layer, the Material Properties is normally characterized by resilient modulus which founded after analysis the pavement structure. The proprieties of the asphaltic concrete layer were taken according to Ramadan [13].

The estimation of the rutting parameters, intercept “a” and slop “b” is obtained from the regression analysis of the linear portion (second stage) of the permanent deformation curve. These two parameters were then used to determine permanent deformation parameters, α (alpha) and μ (gnu), using Eqs.3. These two parameters were then used in the VESYS modelling program to determine the amount of rutting that is expected to occur. A summary of the calculated values for these parameters is given in Table 7.

VESYS Rutting Model Results

As explained, the VESYS model was used to predict the amount of rutting that is expected to occur in a pavement system constructed with the five pavement structure cases. The various inputs needed for VESYS for the bases are shown in Table 8. To simulation the state of pavement in real life, two temperatures were used; 22°C in winter and 40°C in summer.

Typical output generated by VESYS5W for all pavement structures are shown in Figure 18 through Figure 27. The total rut depth is plotted on a linear scale. In general, the total rut decreased with increasing base thickness for all type of bases. The results produced were similar to the results obtained for the permanent deformation tests; with a large amount of deformation occurring at the start of the test and decreasing thereafter to a near constant value.

Table 7: Summary of Rutting Parameters α and μ for base, subbase and subgrade

Soil	additive	Deviator stress, kPa	a(με)		b		μ		α	
			22°C	40°C	22°C	40°C	22°C	40°C	22°C	40°C
Marl	EA	137.8	491.83	--	0.12	--	0.22	--	0.88	--
		275.8	718.72	--	0.09	--	0.15	--	0.91	--
		413.69	740.42	2098.9	0.11	0.04	0.16	0.16	0.88	0.96
		482.63	958.24	2165.1	0.10	0.05	0.16	0.17	0.91	0.95
		551.58	1204.8	2161.9	0.09	0.06	0.19	0.20	0.91	0.94
	ESA	275.8	7655.2	--	0.05	--	0.98	--	0.95	--
		413.69	7002.2	5790	0.07	0.09	0.97	1.02	0.93	0.91
		482.63	6782	10465	0.11	0.04	1.43	0.72	0.88	0.91
		551.58	6567.0	10639	0.15	0.09	1.74	1.72	0.85	0.91
Sabkha	EA	137.8	1098.7	--	0.3	--	1.22	--	0.70	--
		275.8	11355	--	0.02	--	0.42	--	0.98	--
		413.69	3692.9	7172.5	0.32	0.20	2.16	3.53	0.68	0.8
		482.63	1693.7	2494.8	0.49	0.43	1.41	2.29	0.51	0.57
		551.58	1810.2	1570.5	0.52	0.65	1.49	1.96	0.48	0.35
	ESA	137.8	5430.6	--	0.1	--	1.97	--	0.90	--
		275.8	1431.4	--	0.35	--	1.19	--	0.64	--
		413.69	1635	11578	0.38	0.08	1.17	1.74	0.62	0.92
		482.63	1880.4	13711	0.25	0.07	0.79	1.65	0.75	0.93
		551.58	2813	13245	0.36	0.11	1.6	2.24	0.64	0.89
Dune Sand	EA	137.8	1231.4	--	0.07	--	0.32	--	0.93	--
		275.8	1094.8	--	0.11	--	0.28	--	0.88	--
		413.69	1273.9	645.61	0.19	0.75	0.44	0.38	0.81	0.26
		482.63	625.81	389.94	0.40	0.98	0.41	0.27	0.60	0.02
		551.58	1078.2	1406.1	0.34	0.88	0.57	0.83	0.66	0.12
	ESA	275.8	3083.5	--	0.13	--	0.83	--	0.87	--
		413.69	1771.2	4595.9	0.29	0.07	0.90	0.54	0.71	0.93
		482.63	2428.6	3133.2	0.35	0.11	1.40	0.54	0.65	0.89
		551.58	1888.0	2379.1	0.52	0.14	1.53	0.51	0.48	0.86
Marl		68.9	329.75		0.09		0.07		0.91	
Sabkha		68.9	1576.40		0.08		0.20		0.85	
Dune sand		68.9	7429.60		0.11		1.13		0.89	

Table 8: Pavement Materials' Properties and Input Parameters values for VESYS

Parameters	Subgrade/subbase layer**			Base course lyere						Asphalt layer
				Marl		Sabkha		dune sand		
	Marl	Sabkha	Sand	EA	ESA	EA	ESA	EA	ESA	
				Three layers pavement structure VESYS Parameters at 22.2°C						
$M_{R(Mpa)}$	166	-----	-----	680	685	-----	-----	-----	-----	2551*
μ	0.07	-----	-----	0.193	0.474	-----	-----	-----	-----	0.70*
α	0.91	-----	-----	0.891	0.891	-----	-----	-----	-----	0.44*
				VESYS Parameters at 40°C						
$M_{R(Mpa)}$	166	-----	-----	627.5	645	-----	-----	-----	-----	1320*
μ	0.07	-----	-----	0.193	0.568	-----	-----	-----	-----	0.64*
α	0.91	-----	-----	0.891	0.916	-----	-----	-----	-----	0.40*
				Four layers pavement structure VESYS Parameters at 22.2°C						
$M_{R(Mpa)}$	-----	110	100	680	685	665	650	-----	-----	2551*
μ	-----	0.20	1.13	0.193	0.474	0.946	0.946	-----	-----	0.70*
α	-----	0.85	0.89	0.891	0.817	0.814	0.814	-----	-----	0.44*
				VESYS Parameters at 40°C						
$M_{R(Mpa)}$	-----	110	100	627.5	645	573	620	-----	-----	1320*
μ	-----	0.20	1.13	0.193	0.568	4.052	0.637	-----	-----	0.64*
α	-----	0.85	0.89	0.891	0.916	0.814	0.814	-----	-----	0.40*
Thickness (mm)	Infinity/150mm			Variable		Variable		----		100
ν	0.35			0.35		0.35		----		0.35

. *These values after Ramadhan [13] , **Subgrade layer materials were tested at one temperature 22°.

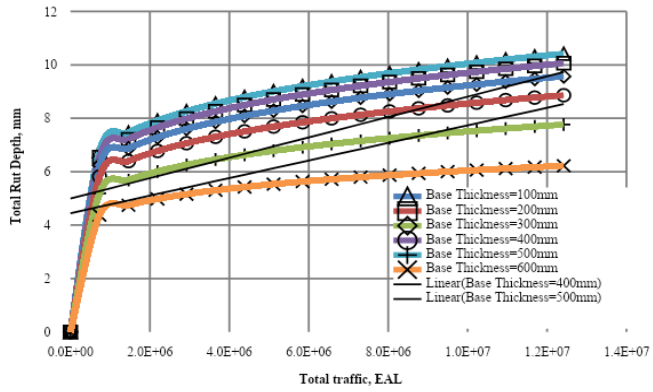

Figure 18: Relation between rut depth and total traffic with effect of base thickness for pavement structure on marl subgrade with marl emulsified sulfur asphalt base.

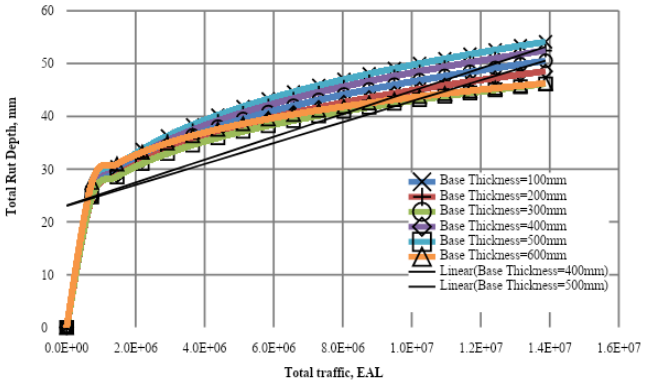

Figure 19: Relation between rut depth and total traffic with effect of base thickness for pavement structure on sabkha subgrade with marl emulsified sulfur asphalt base.

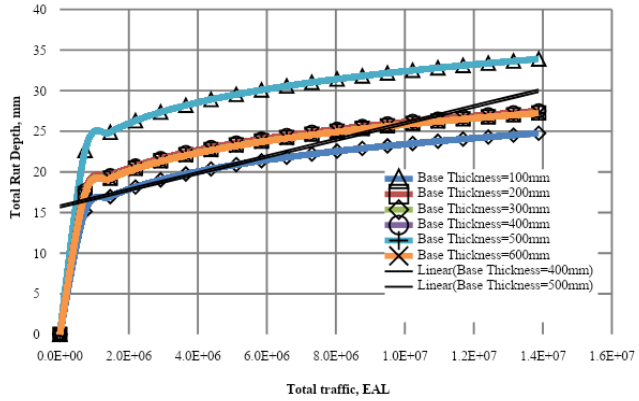

Figure 20: Relation between rut depth and total traffic with effect of base thickness for pavement structure on sabkha subgrade with sabkha emulsified sulfur asphalt base.

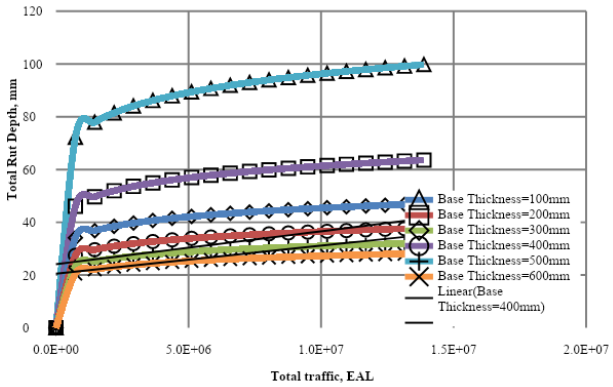

Figure 21: Relation between rut depth and total traffic with effect of full depth thickness for pavement structure on dune sand subgrade with marl emulsified sulfur asphalt base.

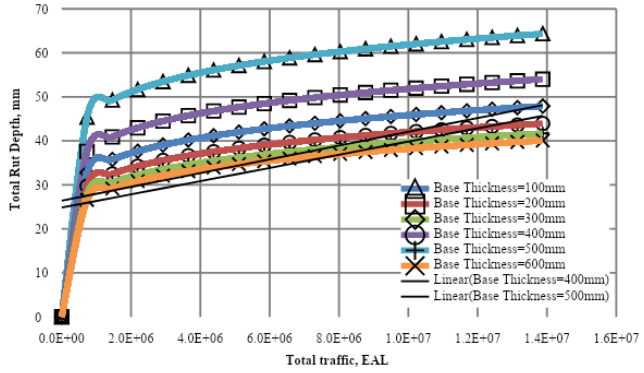

Figure 22: Relation between rut depth and total traffic with effect of base thickness for pavement structure on dune sand subgrade with sabkha emulsified sulfur asphalt base.

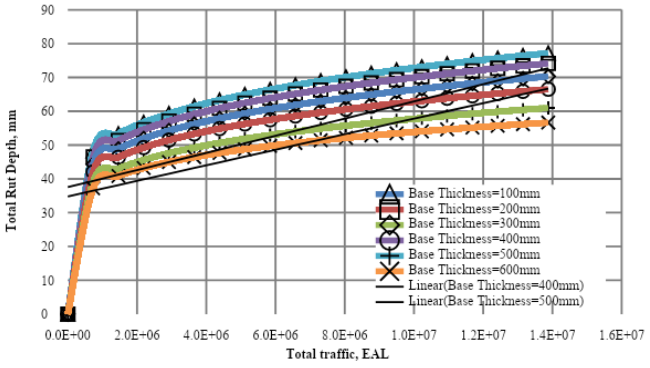

Figure 23: Relation between rut depth and total traffic with effect of base thickness for pavement structure on sabkha subgrade with sabkha emulsion base.

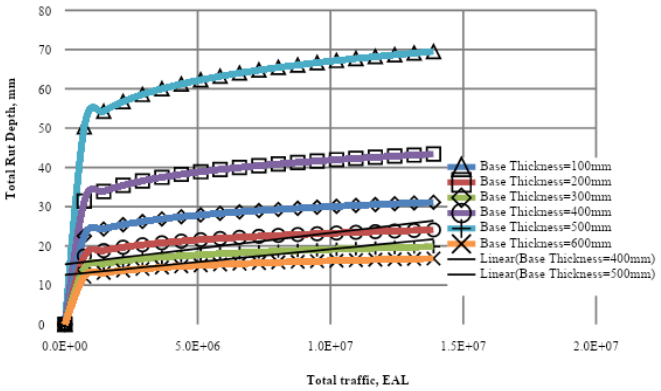

Figure 24: Relation between rut depth and total traffic with effect of full depth thickness for pavement structure on dune sand subgrade with marl emulsion base.

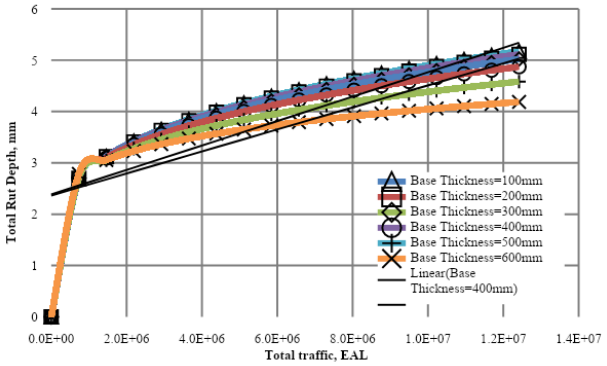

Figure 25: Relation between rut depth and total traffic with effect of base thickness for pavement structure on marl subgrade with marl emulsion base.

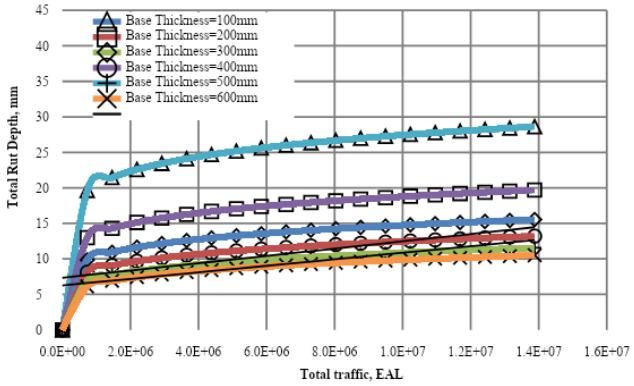

Figure 26: Relation between rut depth and total traffic with effect of base thickness for pavement structure on sabkha subgrade with marl emulsion base.

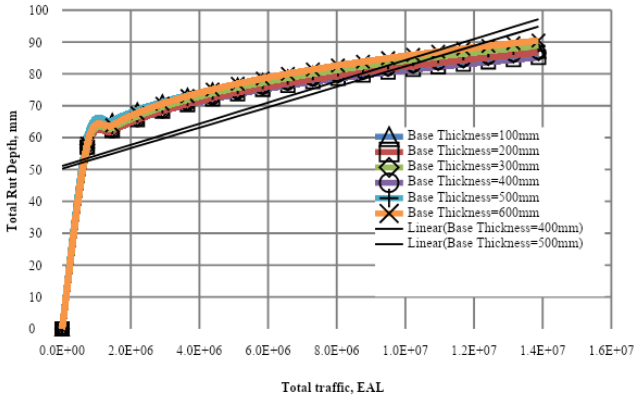

Figure 27: Relation between rut depth and total traffic with effect of base thickness for pavement structure on dune sand subgrade with sabkha emulsion base.

Regression Model Analysis

The statistical analysis of MR has been studied in this work. Table 9 presents the results of ANOVA analysis for resilient modulus. Analysis of MR data using General Linear Model (4-Way analysis, ANOVA) technique, shows that confining stress and deviator stress have a significant effect on MR for marl, sabkha, and dune sand mixes whereas the additive material type has an insignificant effect on MR in three types of soil. Moreover, the temperature has a significant effect on MR for sabkha. This means that the confining stress and deviator stress for all types of treatment soil and temperature for sabkha play a very important role in the resilient modulus when is used to generate the modelling and design pavement structure. On the other hand, temperature has an insignificant effect for marl and dune sand. This means that temperature effect can be neglected when calculating the resilient modulus.

The regression analysis for marl, sabkha and dune sand shows that there is a relationship between resilient modulus (MR) and Temperature, deviator stress, confining Pressure and Type of additives. The best fit was plotted and developed in Appendix A, as it is shown below

$$M_R=166.6 - 2.1T - 35.8S + 9.7A - 0.25\sigma_c + 4.2\sigma_d \quad (5)$$

Where:

M_R = resilient modulus, (MPa), T = Temperature, (^oC), S= Type of soil (Marl=1, Sabkha=2 and Dune sand=3), A= Type of additive (EA=1, ESA=2), σ_c = Confining Pressure, (kPa), and σ_d = Deviator stress, (kPa**)**

The results of statistical analysis for μ and α are shown in Table 9 and Table 10 respectively, for marl, sabkha, and dune sand mixes with EA and ESA. The "F" test results in these Tables show that the deviator stress has an

insignificant effect on the μ and α, with a significance of about 95%. Also, Type of additives has an insignificant effect on α for all soil while, it has a significant effect on μ for marl and dune sand. Moreover the temperature has a significant effect on α marl and μ for sabkha and dune sand while it is an insignificant on Alfa for sabkha and dune sand and μ for marl.

The results of statistical analysis for GNU and ALFA are shown in Table 10 and Table 11 respectively, for marl, sabkha, and dune sand mixes with EA and ESA. The "F" test results in these Tables show that the deviator stress has an insignificant effect on the GNU and ALFA, with a significance of about 95%. Also, Type of additives has an insignificant effect on ALFA for all soil while, it has a significant effect on GNU for marl and dune sand. Moreover the temperature has a significant effect on ALFA marl and GNU for sabkha and dune sand while it is an insignificant on Alfa for sabkha and dune sand and GNU for marl.

The results of regression analysis show that there is a relationship between μ and Type of additives, Temperature and Deviator stress. Also the results show that there is a relationship between α and Type of additives, Temperature and Deviator stress. as it is shown below

Marl $\mu = -1 + X - 0.008\ T + 0.001\ \sigma_d$ (6)

Marl $\alpha = 0.1 - 0.01X + 0.002T + 0.00005\ \sigma_d$ (7)

Sabkha $\mu = 0.7 - 0.3X + 0.05T - 0.0002\ \sigma_d$ (8)

Sabkha $\alpha = 0.5 + 0.15X + 0.007T - 0.0007\sigma_d$ (9)

Dune sand $\mu = 0.03 + 0.4X - 0.02T + 0.001\sigma_d$ (10)

Dune sand $\alpha = 0.9 + 0.2X - 0.007T - 0.001\sigma_d$ (11)

Where: μ = GNU, α = ALFA, T = Temperature, (^oC), X= Type of additives (EA =1; ESA =2), and σd = Deviator stress, (kPa)

Table 9: Results of Resilient Modulus ANOVA at 5% significance level

	Factors/Additives	Calculated F_{value}	P-value	Comment
Marl	Type of additives EA or ESA	0.54	0.467	Insignificant
	Confining stress	36.30	0.000	Significant
	Deviator stress	167.04	0.000	Significant
	Temperature	4.18	0.045	Insignificant
Sabkha	Type of additives EA or ESA	1.27	0.264	Insignificant
	Confining stress	38.94	0.000	Significant
	Deviator stress	179.51	0.000	Significant
	Temperature	7.18	0.009	Significant
Dune Sand	Type of additives EA or ESA	0.14	0.713	Insignificant
	Confining stress	38.65	0.000	Significant
	Deviator stress	157.88	0.000	Significant
	Temperature	1.43	0.236	Insignificant

Table 10: Results of GNU μ ANOVA at 5% significance level

	Factors/Additives	Calculated F_{value}	P-value	Comment
Marl	Type of additives EA or ESA	57.53	0.000	Significant
	Deviator Stress	1.56	0.274	Insignificant
	Temperature	0.54	0.485	Insignificant
Sabkha	Type of additives EA or ESA	0.87	0.374	Insignificant
	Deviator Stress	1.17	0.387	Insignificant
	Temperature	5.89	0.038	Significant
Dune Sand	Type of additives EA or ESA	7.95	0.023	Significant
	Deviator Stress	1.15	0.398	Insignificant
	Temperature	4.68	0.063	Significant

Table 11: Results of ALFA α ANOVA at 5% significance level

	Factors/Additives	Calculated F_{value}	P-value	Comment
Marl	Type of additives EA or ESA	1.40	0.271	Insignificant
	Deviator Stress	1.17	0.393	Insignificant
	Temperature	5.48	0.047	Significant
Sabkha	Type of additives EA or ESA	3.25	0.105	Insignificant

	Deviator Stress	1.25	0.355	Insignificant
	Temperature	1.77	0.216	Insignificant
Dune Sand	Type of additives EA or ESA	3.92	0.083	Insignificant
	Deviator Stress	0.80	0.558	Insignificant
	Temperature	0.76	0.410	Insignificant

Pavement Thickness Design Charts

This section describes the application of results of rutting modeling, conducted as described, in the design of pavement systems employing EA and ESA with local soils (i.e., marl, sabkha, and dune sand) as base courses. The 25 mm rut depth was used as critical rutting to compute the limit number of load repetitions from rut depth curves which led to the development of design charts for variable thickness of base between 100 mm to 600 mm. After that, Relations between base thickness and total traffic for each rut depth were plotted [14].

Figure 28 through Figure 37 show pavement lives predicted to achieve a certain rut depth for pavement structure cases. The design charts were developed for two seasons, the first when materials at 22^{o}C in the winter and the second when materials at 40^{o}C in the summer.

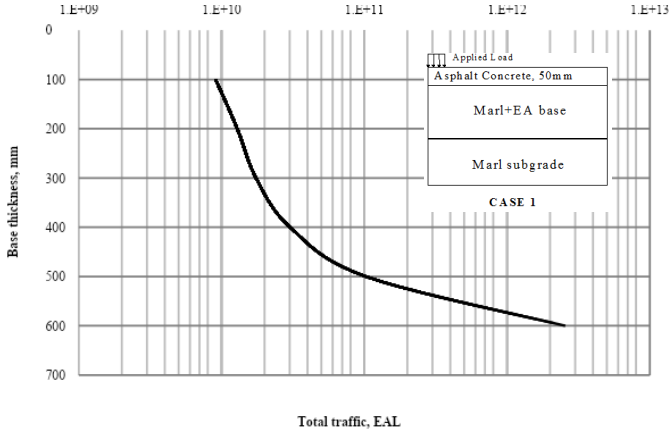

Figure 28: Relation between marl with EA base thickness and total traffic (case 1).

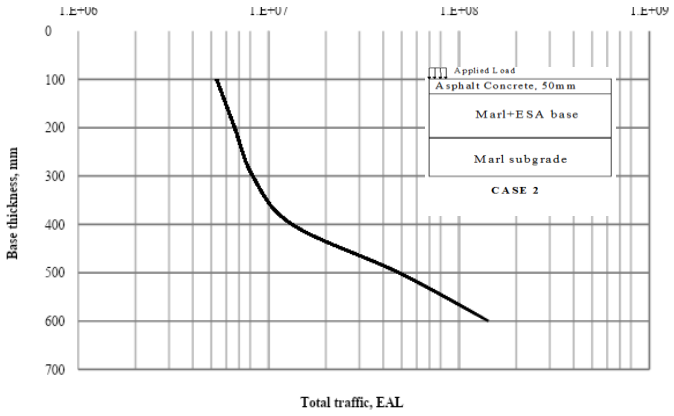

Figure 29: Relation between marl with ESA base thickness and total traffic for (case 2).

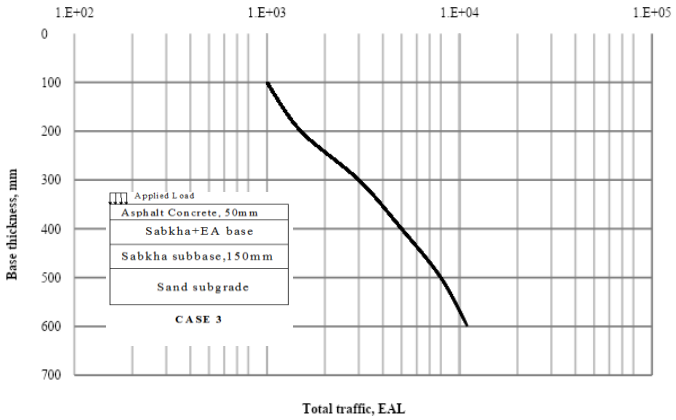

Figure 30: Relation between sabkha with EA base thickness and total traffic (case 3)

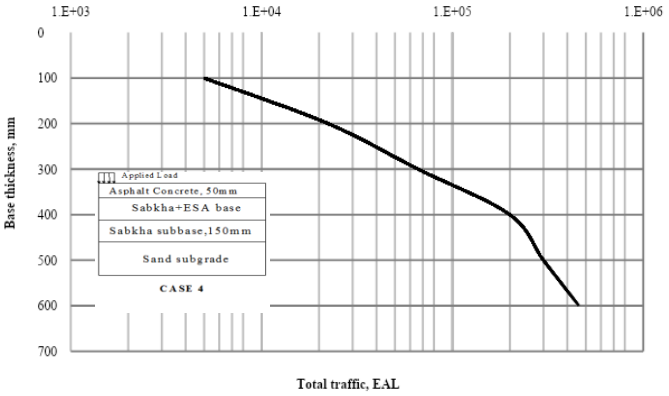

Figure 31: Relation between sabkha with ESA base thickness and total traffic (case 4)

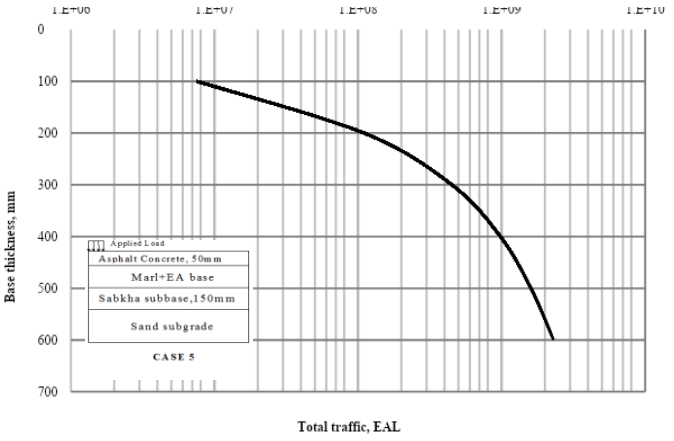

Figure 32: Relation between marl with EA base thickness and total traffic (case 5)

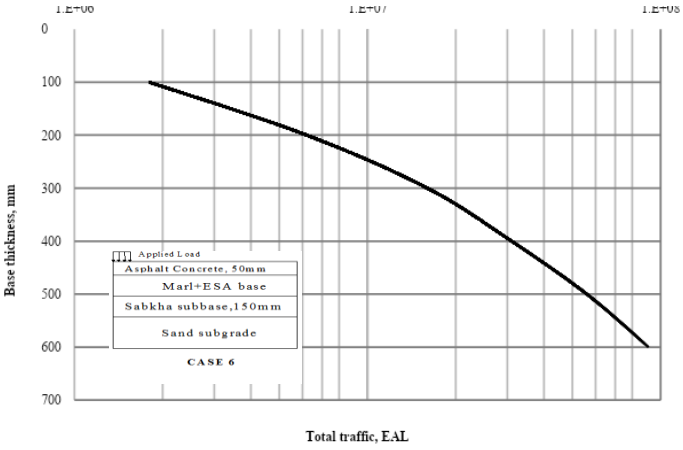

Figure 33: Relation between marl with ESA base thickness and total traffic (case 6)

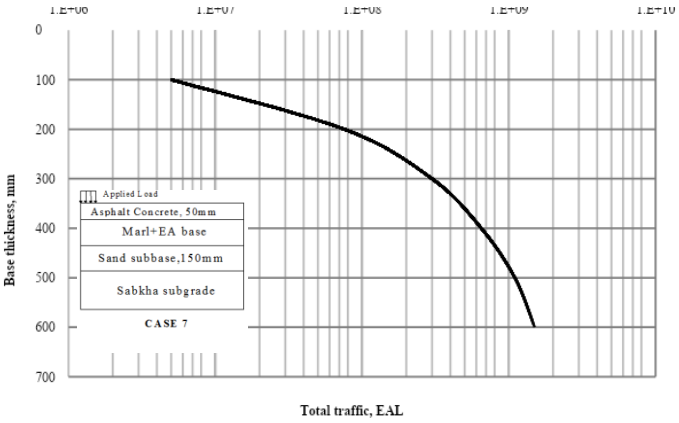

Figure 34: Relation between marl with EA base thickness and total traffic (case 7)

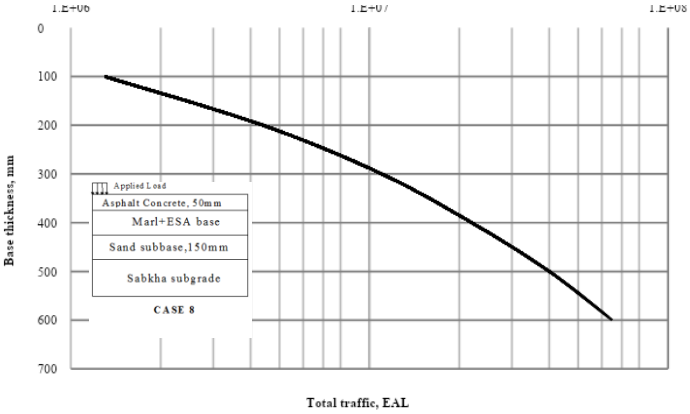

Figure 35: Relation between marl with ESA base thickness and total traffic (case 8)

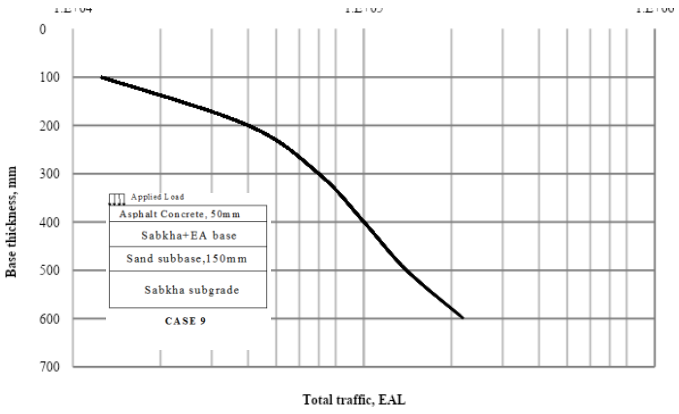

Figure 36: Relation between sabkha with EA base thickness and total traffic (case 9)

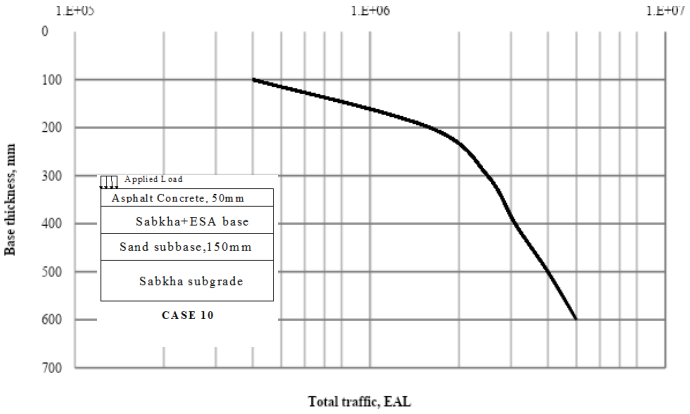

Figure 37: Relation between marl with ESA base thickness and total traffic (case 10)

Conclusions

Summary of the general findings from the results analysis were presented in the subsequent sub-heading, test-wise. Based on the graphical and statistical interpretation of the data obtained from the various test conducted, the trend and manner in which the different additives (EA and ESE) affect each property were highlighted.

1. Dune sand did not satisfy the minimum requirement of ITS so it was not used as base for constriction roads.
2. Permanent deformation results showed that in general, permanent strain and resultant strain increased with increases in deviatoric stress.
3. In the general values of α decreased with increases in deviatoric stress because of increasing of permanent deformation slop. On the other hand, the values for μ increased with increases in deviatoric stress.
4. The lower the resilient modulus the higher the permanent deformation exhibited will be in the material under repeated loading.
5. VESYS predictions of rut depth follow similar patterns as those found in the permanent deformation tests.
6. Both permanent deformation test and VESYS can be said to be good indicators of how a base material will perform under traffic loads.
7. Marl and sabkha with emulsified asphalt can be used for road construction.
8. Marl emulsified asphalt mixes tend to withstand higher loads with low rutting (5mm) than dune sand and sabkha with emulsified asphalt.
9. Three local soils (marl, dune sand and sabkha) treated with EA mixes at two temperatures (22 ºC and 40 ºC) were considered for analyzing with VESYS5W program.
10. The rutting criteria were used to develop pavement structure design charts. These design charts can be used under the same specification for local streets in Saudi Arabia.

References

[1]. Al-Abdulwahhab, H.I., *Evaluation of emulsified asphalt for use in Saudi Arabia*. 1985, Oregon State Univ., Corvallis (USA).
[2]. Garba, R., *Permanent deformation properties of asphalt concrete mixtures.* 2002.
[3]. ASTM, *Annual book of ASTM Standards*. 2004, American Society for Testing & Materials.
[4]. AEMA, *19-A Basic Asphalt Emulsion Manual*. 2004, The Asphalt Institute and the Asphalt Emulsion Manufacture's Association.
[5]. AASHTO, M., *M 43-88 (2003)"Standard Specification for Sizes of Aggregates for Road and Bridge Construction" AASHTO Standard Specifications for Transportation Materials and Methods of Sampling and Testing*, in *Washington, DC*. 2004.
[6]. Werkmeister, S., A.R. Dawson, and F. Wellner, *Permanent deformation behavior of granular materials and the shakedown concept.* Transportation Research Record: Journal of the Transportation Research Board, 2001. **1757**(1): p. 75-81.
[7]. Asphalt. Institute, *Development of the Asphalt Institute thickness design manual (MS-1)*. 1982, Research Report No. 81-2 (RR-81-2).
[8]. Moavenzadeh, F., J. Soussou, and H. Findakly, *Synthesis for rational design of flexible pavements*. 1974: Department of Transportation, Federal Highway Administration, Office of Research and Development.
[9]. Vijayaruban, N. *Development of Pavement Performance Evaluation Subroutines for 3D-Move Analysis Software*. in *Masters Abstracts International*. 2011.
[10]. Zhou, F. and T. Scullion, *Asphalt Pavement Performance Analysis Tool: TTI VESYS5W*. 2006, Texas Transportation Institute, Texas A&M University System.
[11]. Rogers, M., *Highway engineering*. 2003: Blackwell Publishing.
[12]. Heukelom, W. and A. Klomp. *Dynamic testing as a means of controlling pavements during and after construction*. in *International conference on the structural design of asphalt pavements*. 1962.
[13]. Ramadhan, R.H., *Prediction of pavement rutting from laboratory characterization tests.* Civil Engineering, 1988. 10: p. 04-1988.
[14]. Arnold, G. and S. Werkemeister, *Pavement thickness design charts derived from a rut depth finite element model*. 2010.